p-ISSN: 2614-8897

SEGMENTATION OF SUBARACHNOID HEMORRHAGE ON BRAIN CT IMAGES USING U-NET AND ATTENTION U-NET: A COMPARATIVE ANALYSIS

Ilham Tristadika Saputra^{1*}, Afu Ichsan Pradana², Dwi Hartanti³

^{1,2,3}Sistem Informasi, Fakultas Ilmu Komputer, Duta Bangsa University, Surakarta, Indonesia Email: *1210103020@mhs.udb.ac.id, ²afu ichsan@udb.ac.id, ³dwihartanti@udb.ac.id

(Received: 27 May 2025, Revised: 10 June 2025, Accepted: 28 June 2025)

Abstract

Subarachnoid Hemorrhage (SAH) represents a critical medical condition resulting from bleeding in the subarachnoid space, typically due to the rupture of an aneurysm or trauma. Timely identification is vital to avoid long-term neurological impairment. This research assesses the efficacy of U-Net compared to Attention U-Net for the segmentation of SAH in brain CT images, aiming to determine if attention mechanisms enhance segmentation precision. The motivation for this comparison stems from the clinical difficulty in identifying subtle or low-contrast hemorrhagic areas that traditional architectures like U-Net might miss; in contrast, attention-based models are constructed to capture spatial details more proficiently. Both architectures were evaluated using a publicly available SAH CT dataset and assessed on metrics including Dice Score, Intersection over Union (IoU), Precision, Recall, and F1 Score. Attention U-Net outperformed U-Net with higher scores of Dice (0.896) and IoU (0.877), whereas U-Net excelled in precision. Visual assessments also indicated that Attention U-Net was superior in delineating diffuse hemorrhagic regions. These findings advocate for the incorporation of attention mechanisms to enhance segmentation accuracy and clinical relevance in neuroimaging.

Keywords: Subarachnoid Hemorrhage, Brain CT Scan, Medical Image Segmentation, U-Net, Attention U-Net, Dice Score

This is an open access article under the **CC BY** license.



*Corresponding Author: Ilham Tristadika Saputra

1. INTRODUCTION

Subarachnoid Hemorrhage (SAH) is a critical neurological condition involving bleeding in the subarachnoid space, typically triggered by a ruptured cerebral aneurysm or significant head injury [1]. SAH represents around 5% of all stroke occurrences and impacts between 2 to 25 adults per 100,000 personyears in those over 35, with a greater frequency observed in females. [1], [2]. Due to its sudden onset and potentially devastating consequences—including coma, long-term disability, or death—early and accurate identification is not just important, but a responsibility that can significantly improve clinical outcomes [3].

Computed Tomography (CT) is the most widely used imaging modality for initial SAH assessment, primarily because of its rapid acquisition, non-invasiveness, and high sensitivity to acute hemorrhage during the first 72 hours [4]. However, the interpretation of CT scans, despite its widespread use,

is not without its limitations. It relies heavily on the expertise of radiologists and is prone to subjectivity. Manual segmentation of hemorrhagic areas can be time-consuming. suffers from inter-observer variability, and is particularly challenging when segmenting low-contrast or small-volume hemorrhages [5], [6]. These limitations, which can potentially affect patient outcomes, highlight the urgent need for automated, reproducible, and efficient tools for hemorrhage localization and delineation to support clinical workflows.

In the past few years, methods based on deep learning have transformed the analysis of medical images, especially in semantic segmentation tasks that employ convolutional neural networks (CNNs). A comprehensive review by Litjens et al. reinforces this trend by highlighting how deep learning has advanced various medical imaging tasks, including detection, classification, and segmentation [7]. Among them, U-Net has emerged as a benchmark architecture due to its encoder-decoder structure and skip connections,

which facilitate both global context and fine-detail localization [8]. While effective in many applications, standard U-Net architectures often struggle to segment small or diffuse lesions, such as SAH, where the boundaries between hemorrhagic and healthy tissues can be subtle and poorly defined [9].

Recent developments have also focused on enhancing segmentation performance through semisupervised learning and transfer learning techniques [10]. However, these approaches may require substantial computational resources or pre-trained encoders, prompting interest in lightweight yet effective models like U-Net and its attention-based variants.

Attention-based models, first made popular in natural language processing by Vaswani et al. [11], have shown considerable advantages in biomedical image segmentation by enabling the network to concentrate on anatomically relevant areas. The Attention U-Net incorporates attention gates (AGs) at skip connections, which facilitate dynamic feature filtering and highlight important regions of the image while minimizing background interference [12], [13]. Research conducted by Yang and Jin [14] further reinforces the importance of attention mechanisms in enhancing segmentation accuracy, particularly in intricate CT imaging scenarios characterized by anatomical uncertainty.

Previous research has explored the use of deep learning models in medical image segmentation, particularly for brain abnormalities. Chang et al. [15] employed an Attention U-Net architecture to segment intracranial hemorrhages from CT images, showing notable improvement in segmentation accuracy through attention mechanisms. However, their study did not focus specifically on subarachnoid hemorrhage (SAH), which presents unique challenges due to its subtle and diffuse characteristics. In contrast, this study is a novel exploration that concentrates exclusively on SAH segmentation. It compares the performance of both U-Net and Attention U-Net architectures, offering a more targeted evaluation relevant to emergency neuroimaging.

Suta et al. [16] conducted segmentation on brain tumors using U-Net applied to MRI images, achieving improved accuracy in neoplastic detection. However, their work did not address hemorrhagic lesions or use CT-based data, which is the standard modality for acute SAH diagnosis. Our approach differs by focusing on hemorrhagic segmentation using CT scans, specifically within the subarachnoid space, making it more applicable in clinical settings.

This study presents a focused comparative analysis of SAH segmentation, highlighting the impact of attention mechanisms on enhancing spatial precision and segmentation effectiveness. Beyond performance improvements, the results also carry practical relevance—particularly in addressing challenges associated with low-contrast hemorrhagic regions, which are often misinterpreted using traditional analysis methods. By improving the detection of such subtle features, this approach has the potential to enhance the reliability of emergency neuroimaging. In line with this direction, recent national studies such as that by Prasetyo [17] have explored similar applications of machine learning, demonstrating promising results in brain tumor detection using MRI data.

This paper is structured as follows: Section 2 provides a summary of the dataset, covering the preprocessing steps and the experimental framework. Section 3 details the model architectures and the parameter configurations employed. Section 4 presents the evaluation outcomes, which are analyzed in greater depth in Section 5. Finally, Section 6 wraps up the study and suggests potential avenues for future research.

2. RESEARCH METHOD

This study was conducted through several key stages, including data preparation, model architecture design, training procedure, and performance evaluation. The research methodology workflow used in this study can be represented in Figure 1.

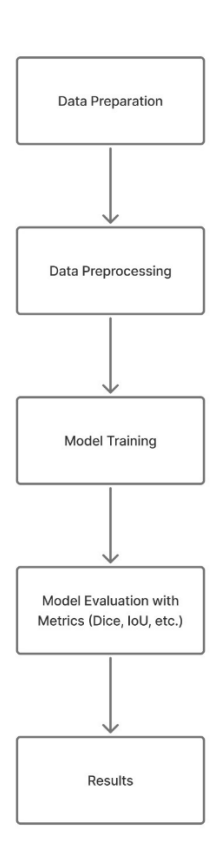


Figure 1. Workflow of the proposed SAH segmentation system using U-Net and Attention U-Net.

2. 1 Dataset Preparation

The dataset employed in this study was retrieved from Roboflow Universe [18] and serves as a valuable public resource containing CT scan images annotated for subarachnoid hemorrhage (SAH) segmentation. Each image includes a binary mask highlighting hemorrhagic regions. An example of the paired input and corresponding output mask is presented in Figure 2. The dataset is distributed under the Creative Commons Attribution 4.0 International (CC BY 4.0) license, which permits unrestricted use for research purposes, enabling further exploration and analysis of SAH cases.

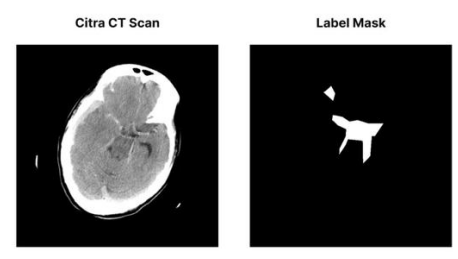


Figure 2. CT scan image and corresponding binary label mask

The dataset was split into training, validation, and testing sets. The training subset was employed to adjust the model's internal parameters, whereas the validation set was utilized to monitor performance and optimize hyperparameters during the learning process. The testing set was designated to evaluate the model's ability to generalize to new, unseen data. To ensure consistent class distribution in all partitions, stratified sampling was used.

2. 2 Data Preprocessing

Preprocessing was performed via a custom dataset class that automatically loads image-mask pairs. CT images were loaded in grayscale using OpenCV, scaled to 256×256 pixels through interpolation, and resized using nearest-neighbor interpolation to preserve their binary accuracy [5], [9]. Pixel values were normalized to the [0,1] range by dividing by 255. Masks were binarized with a threshold of 0.5. Both images and masks were converted into PyTorch-compatible tensors with shapes [1, H, W]. This preprocessing pipeline was integrated directly into the DataLoader to enhance training efficiency and ensure reproducibility, following the design described by El Abassi et al. [13]. In addition, basic data augmentation techniques such as horizontal flips and random rotation were applied during training to enhance model robustness and reduce overfitting, in line with standard practices in medical image analysis [1], [19].

2. 3 Model Architecture

This research utilized two models for semantic segmentation: U-Net and Attention U-Net. U-Net features a symmetrical architecture comprising an encoder and decoder, improved by skip connections that aid in maintaining spatial features. The encoder was enhanced using ResNet34 as a backbone to improve feature representation via residual learning,

which also aids gradient stability and convergence during training [8].

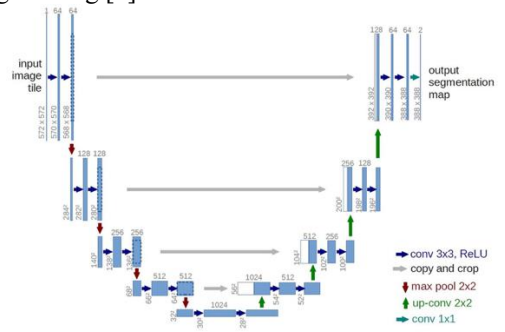


Figure 3. U-Net architecture adopted from [8].

Attention U-Net incorporates attention gates (AGs) within the skip connections that link the encoder and decoder layers. These gates are designed to suppress irrelevant spatial features while enhancing focus on the most informative regions associated with the target area (SAH). This mechanism increases the model's responsiveness to small or low-contrast regions by adaptively emphasizing meaningful activations [12]. Figures 3 and 4 visualize the architectural designs of both models.

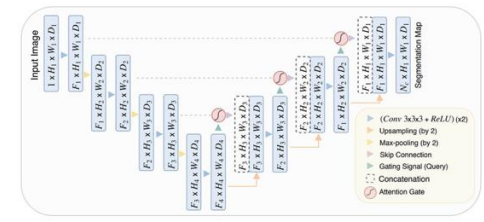


Figure 4. Attention U-Net architecture adapted from [12]

2. 4 Training Procedure

The entire model training process took place on Google Colab with the assistance of an NVIDIA A100 GPU. Prior to inputting the CT scan images and their associated segmentation masks into the models, they were resized to 256 × 256 pixels and normalized within a range of [0, 1]. Both U-Net and Attention U-Net architectures were developed in PyTorch, employing ResNet-34 as the encoder backbone to enhance feature extraction.

The training procedure was carried out for 40 epochs with a batch size of 16, utilizing the Adam optimizer and starting with a learning rate 1e-4. The model employed a combined loss function of Binary Cross-Entropy (BCE) and Dice Loss to ensure a balance between pixel-level prediction precision and segmentation overlap. The model version that recorded the highest Dice Score on the validation dataset was chosen for the final assessment. To ensure fair comparison of architectures, no pre-trained weights or transfer learning methods were used.

2. 5 Evaluation Metrics

The segmentation outcomes were assessed quantitatively on the test dataset using five metrics: Dice Score, Intersection over Union (IoU), Precision,

Recall, and F1 Score. The Dice Score quantifies the spatial agreement between the predicted and ground truth masks and is calculated using Formula 1.

$$Dice = \frac{2 \times (|P \cap G|)}{(|P| + |G|)} \tag{1}$$

Intersection over Union (IoU) quantifies the agreement between prediction and ground truth masks relative to their union and is defined by Formula 2.

$$IoU = \frac{(|P \cap G|)}{(|P \cup G|)} \tag{2}$$

Where *P* is the predicted binary mask, and *G* is the ground truth mask. These metrics provide comprehensive insight into segmentation accuracy, robustness, and consistency.

3. RESULT AND DISCUSSION

3. 1 Dataset Preparation

The visualization of training dynamics for both model architectures-U-Net and Attention U-Netdemonstrates that convergence was achieved within a relatively efficient training period. The trends observed in both training and validation loss curves exhibit consistent reductions, indicating that the models did not experience significant overfitting during the learning phase.

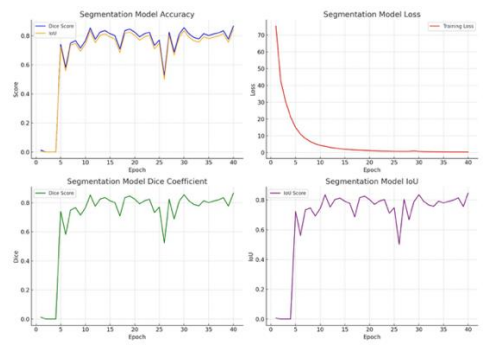


Figure 5. Training performance visualization of the U-Net model

As illustrated in Figure 5, the U-Net model exhibits a consistent and rapid reduction in both training and validation losses, starting from the early epochs. The loss trajectories indicate stable convergence, with minimal disparity between training and validation performance—suggesting that the model is capable of generalizing well to unseen data.

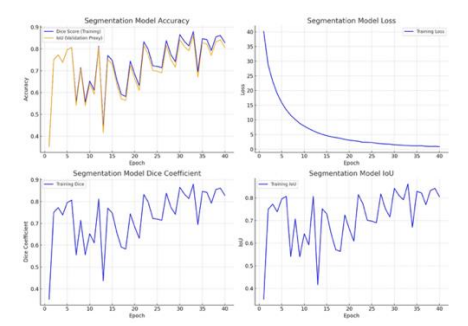


Figure 6. Training performance visualization of the Attention U-Net model

Conversely, the Attention U-Net model (Figure 6) reveals more fluctuation in loss values during the initial training phase and requires a longer duration to attain stabilization. Nevertheless, the later epochs indicate a convergence trajectory similar to that of U-Net, affirming that despite its increased architectural the optimization process remains complexity. effective.

Overall, both models exhibit stable and reliable convergence behaviors. The U-Net architecture demonstrates faster stabilization, whereas Attention U-Net, although slower to stabilize, ultimately aligns to a consistent performance pattern. These results indicate that both segmentation models possess adequate learning capacity and robustness in training for SAH segmentation tasks.

3. 2 Segmentation Output Visualization

To demonstrate the reliable spatial performance of both models, Figure 7 presents segmentation results from three representative brain CT scan samples. Each row displays a sample composed of four columns: the original CT scan with ground truth annotation (red contour), the prediction map from the U-Net model, the prediction map from the Attention U-Net model, and the binary ground truth mask for comparison.

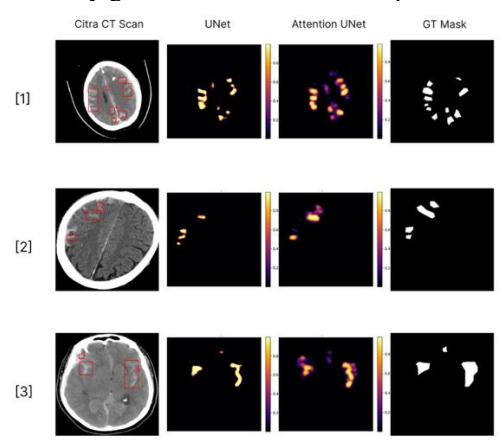


Figure 7. Visual comparison of segmentation results by U-Net and Attention U-Net models

U-Net detected most of the hemorrhagic region in the preliminary sample, achieving a Dice Score of 0.59 and IoU of 0.42. The Attention U-Net achieved a slightly elevated Dice Score of 0.61, an IoU of 0.44, and a Recall of 0.69, indicating an improved capacity to identify the target area.

In the second sample, where the SAH region was smaller, U-Net produced high precision (0.70) but low recall (0.31). Attention U-Net improved recall to 0.44 and Dice Score to 0.49 (compared to U-Net's 0.43), demonstrating its advantage in identifying small, localized structures. In the third sample, both models produced consistent predictions. U-Net recorded a Dice Score of 0.67 and IoU of 0.51, while Attention U-Net outperformed with a Dice Score of 0.73 and IoU of 0.57. These findings suggest that although both models approximate the ground truth with high

accuracy, Attention U-Net consistently maintains a better metric balance.

Overall, the combined visualizations in Figure 7 indicate that U-Net excels in broader region coverage. In contrast, Attention U-Net demonstrates superior spatial accuracy and sensitivity, especially in identifying smaller and more diffuse SAH regions.

3. 3 Quantitative Performance Evaluation per Sample

Table 1 presents the quantitative evaluation results based on six primary metrics and the percentage of segmented areas. To enhance clarity, the performance metrics of the U-Net model are displayed first, followed by those of the Attention U-Net. This arrangement allows for a structured and thorough comparison between the two models in segmenting subarachnoid hemorrhage (SAH) regions within brain CT scans.

Table 1. Quantitative evaluation of U-Net model on selected

samples.					
Metric	Sample 1	Sample 2	Sample 3		
Dice Score	0.57	0.57	0.73		
IoU	0.39	0.40	0.57		
Precision	0.50	0.79	0.81		
Recall	0.65	0.45	0.66		
F1 Score	0.57	0.57	0.73		
Area %	3.35%	1.1%	2.76%		

The U-Net model shows relatively consistent performance across the three samples, with the highest Dice Score of 0.73 achieved on the third sample and the largest predicted segmentation area (3.35%) observed in the first. The model also demonstrates strong recall across samples, indicating good sensitivity toward the target region, although some trade-offs with lower precision are noted.

Table 2. Quantitative evaluation of Attention U-Net model on

selected samples.				
Metric	Sample 1	Sample 2	Sample 3	
Dice Score	0.57	0.57	0.73	
IoU	0.39	0.40	0.57	
Precision	0.50	0.79	0.81	
Recall	0.65	0.45	0.66	
F1 Score	0.57	0.57	0.73	
Area %	3.35%	1.1%	2.76%	

In contrast, the Attention U-Net model displays greater variability across the samples. In the first sample, it recorded a Dice Score of 0.61 and a Recall of 0.69, reflecting the model's capacity to detect dispersed SAH areas. In the second sample, though, performance decreased, resulting in a Dice Score of 0.38 and an IoU of 0.23. This suggests that spatial attention mechanisms, although effective, may not yet fully optimize performance for detecting very small or low-contrast structures.

3. 4 Aggregate Performance Comparison

Figure 8 presents representative slices from the test dataset used for aggregate evaluation. This visualization provides context on the diversity of SAH

cases encountered, as well as the spatial complexity faced by the segmentation models.

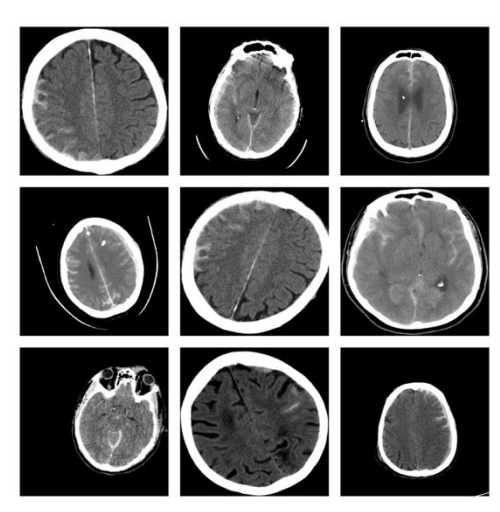


Figure 8. Representative brain CT scan slices from the test dataset

Subsequently, Table 3 presents the aggregate performance metrics of both models evaluated on the entire test set consisting of 86 batches. The evaluation utilizes five main metrics: Dice Score, IoU, Precision, Recall, and F1 Score. This table facilitates a direct comparison between U-Net and Attention U-Net in terms of global segmentation performance. U-Net demonstrates a higher precision (0.725), reflecting its tendency to avoid over-segmentation. On the other hand, Attention U-Net records higher scores in Dice (0.896), IoU (0.877), and Recall (0.557), indicating stronger sensitivity in capturing subarachnoid hemorrhage areas.

Table 3. Comparative evaluation metrics of U-Net and Attention

U-Net on the full test set.				
Metric	U-Net	Attention U-Net		
Dice Score	0.867	0.896		
IoU	0.848	0.877		
Precision	0.725	0.637		
Recall	0.478	0.557		
F1 Score	0.507	0.553		

Overall, this comparison reinforces that Attention U-Net is more suitable for scenarios requiring broad coverage and high sensitivity to small structures. In contrast, U-Net may be preferable when the clinical focus is on precision and background noise suppression. These findings support earlier samplebased analyses and justify selecting models according to specific clinical or operational priorities.

Figure 9 displays a bar chart comparison of the aggregated evaluation metrics for U-Net and Attention U-Net. This visualization further substantiates the tabulated quantitative findings, clearly illustrating each model's relative strengths. Attention U-Net outperforms in Dice, IoU, and Recall, while U-Net leads in Precision. Such differences suggest model selection should align with segmentation objectives, whether for comprehensive detection or targeted Precision.

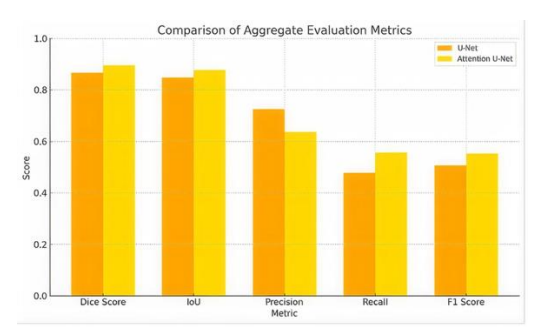


Figure 9. Visualization comparing evaluation metrics between U-Net and Attention U-Net.

3. 5 Analysis and Interpretation of Results

The findings obtained from both per-sample and full-dataset evaluations indicate that U-Net and Attention U-Net each exhibit distinct advantages in the Subarachnoid Hemorrhage (SAH) segmentation. On aggregate evaluation, the Attention U-Net model achieved a Dice Score of 0.896 and an IoU of 0.877, slightly outperforming the U-Net model, which recorded a Dice Score of 0.867 and an IoU of 0.848. However, U-Net demonstrated higher precision (0.725 versus 0.637), indicating a tendency toward more conservative and less noisy predictions. Conversely, the higher recall of Attention U-Net (0.557 versus 0.478) reflects its stronger ability to identify SAH regions more comprehensively.

Visual inspection of segmentation outputs supports the quantitative findings. On samples with smaller and scattered SAH regions, Attention U-Net yielded more spatially accurate results. In contrast, U-Net performed better in detecting larger hemorrhagic areas, albeit sometimes including irrelevant regions. In general, both models demonstrated competent segmentation performance with complementary characteristics. Attention U-Net is more responsive to irregular and dispersed hemorrhages, while U-Net offers better local precision. These distinctions suggest that model selection should be aligned with the specific objectives of the target segmentation system.

4. CONCLUSION

This study conducted a comparative analysis between U-Net and Attention U-Net architectures for segmenting subarachnoid hemorrhage (SAH) regions on brain CT images. The results demonstrate that while both models exhibit competent segmentation performance, the Attention U-Net consistently outperforms the standard U-Net in terms of Dice Score (0.896 vs 0.867), IoU (0.877 vs. 0.848), and Recall (0.557 vs 0.478). Conversely, U-Net achieved higher Precision (0.725), indicating a more conservative segmentation approach. These findings suggest that attention mechanisms enhance spatial sensitivity, especially for detecting subtle or low-contrast hemorrhagic areas.

The findings of this study highlight the potential of Attention U-Net for implementation in clinical decision support tools, particularly in emergency

neuroimaging settings where rapid and accurate analysis is crucial. Prospective research may include expanding the segmentation task to handle multiple types of hemorrhages, exploring transformer-based network designs, and conducting evaluations on larger, cross-institutional datasets further to validate the model's generalizability and clinical applicability.

REFERENCE 5.

- [1] C. Shorten and T. M. Khoshgoftaar, "A survey on Image Data Augmentation for Deep Learning," J Big Data, vol. 6, no. 1, p. 60, Dec. 2019, doi: 10.1186/s40537-019-0197-0.
- [2] N. M. Dubosh and J. A. Edlow, "Diagnosis and Initial Emergency Department Management of Subarachnoid Hemorrhage," Emerg Med Clin North Am, vol. 39, no. 1, pp. 87–99, Feb. 2021, doi: 10.1016/j.emc.2020.09.005.
- [3] A. Arab et al., "A fast and fully-automated deeplearning approach for accurate hemorrhage segmentation and volume quantification in noncontrast whole-head CT," Sci Rep, vol. 10, no. 1, p. 19389, Nov. 2020, doi: 10.1038/s41598-020-76459-7.
- [4] Y. Yu, M. Li, L. Liu, Y. Li, and J. Wang, "Clinical big data and deep learning: Applications, challenges, and future outlooks," Big Data Mining and Analytics, vol. 2, no. 4, pp. 288-305, Dec. 2019, doi: 10.26599/BDMA.2019.9020007.
- [5] S. Umapathy, M. Murugappan, D. Bharathi, and Thakur, "Automated Computer-Aided Detection and Classification of Intracranial Hemorrhage Using Ensemble Deep Learning Techniques," Diagnostics, vol. 13, no. 18, p. 2987, Sep. 2023, doi: 10.3390/diagnostics13182987.
- [6] M. D. Hssayeni, M. S. Croock, A. D. Salman, H. F. Al-khafaji, Z. A. Yahya, and B. Ghoraani, "Intracranial Hemorrhage Segmentation Using a Deep Convolutional Model," Data (Basel), vol. 5, no. 1, p. 14, Feb. 2020, doi: 10.3390/data5010014.
- [7] G. Litjens et al., "A survey on deep learning in medical image analysis," Med Image Anal, vol. 60-88, Dec. 2017, pp. 10.1016/j.media.2017.07.005.
- [8] O. Ronneberger, P. Fischer, and T. Brox, "U-Net: Convolutional Networks for Biomedical Image Segmentation," May 2015.
- [9] M. M. Khan et al., "A Deep Learning-Based Automatic Segmentation and 3D Visualization Technique for Intracranial Hemorrhage Detection Computed Tomography Diagnostics, vol. 13, no. 15, p. 2537, Jul. 2023, doi: 10.3390/diagnostics13152537.
- [10] L. Dai, Md Gapar Md Johar, and Mohammed Hazim Alkawaz, "Review of Semi-Supervised Medical Image Segmentation based on the U-Net," Academic Journal of Science and

- Technology, vol. 11, no. 1, pp. 147-154, May 2024, doi: 10.54097/gmhkht38.
- [11] A. Vaswani et al., "Attention is All you Need," in Advances in Neural Information Processing Systems, I. Guyon, U. Von Luxburg, S. Bengio, H. Wallach, R. Fergus, S. Vishwanathan, and R. Garnett, Eds., Curran Associates, Inc., 2017. [Online]. https://proceedings.neurips.cc/paper files/paper/ 2017/file/3f5ee243547dee91fbd053c1c4a845aa-Paper.pdf
- [12] O. Oktay et al., "Attention U-Net: Learning Where to Look for the Pancreas," Apr. 2018.
- [13] F. El Abassi, A. Darouichi, and A. Ouaarab, "Comparative Analysis of U-Net with Transfer Learning and Attention Mechanism for Enhanced Medical Image Segmentation," 2024, pp. 551-560. doi: 10.1007/978-3-031-68653-5 52.
- [14] X. L. Yang and Z. Y. Jin, "Att GGO-Net:A Semantic Segmentation Method of Lung CT Images with Self and Cross Attention Mechanism," J Phys Conf Ser, vol. 2504, no. 1, p. 012017, May 2023, doi: 10.1088/1742-6596/2504/1/012017.
- [15] C. S. Chang, T. S. Chang, J. L. Yan, and L. Ko, "All Attention U-NET for Semantic Segmentation of Intracranial Hemorrhages In Head CT Images," 2023. 10.1109/BioCAS54905.2022.9948588.
- [16] I. B. L. M. Suta, M. Sudarma, and I. N. Satya Kumara, "Segmentasi Tumor Otak Berdasarkan Citra Magnetic Resonance Imaging Dengan Menggunakan Metode U-NET," Majalah Ilmiah Teknologi Elektro, vol. 19, no. 2, p. 151, Dec. 2020, doi: 10.24843/MITE.2020.v19i02.P05.
- "BRAIN [17] S. Yuda Prasetyo, **TUMOR** DETECTION FROM MRI IMAGES USING DISCRETE COSINE TRANSFORM FEATURES AND EXTREME LEARNING MACHINE," JIKO (Jurnal Informatika dan Komputer), vol. 6, no. 1, pp. 1-6, Apr. 2023, doi: 10.33387/jiko.v6i1.5230.
- [18] Roboflow, "SAHSegmentation Dataset," https://universe.roboflow.com/subarachnoid/sahs egmentation. Accessed: Jun. 17, 2025. [Online]. Available: https://universe.roboflow.com/subarachnoid/sahs egmentation
- [19] S. Tenny, J. Das, and W. Thorell, "Intracranial Hemorrhage - StatPearls - NCBI Bookshelf." Accessed: May 26, 2025. [Online]. Available: https://www.ncbi.nlm.nih.gov/books/NBK47024 2/